Current Applied Physics 14 (2014) 721–724

Contents lists available at ScienceDirect

Current Applied Physics

journal homepage: www.elsevier.com/locate/cap

Transition behaviors in biased asymmetric quantum dot-in-double-well photodetector

H.W. Shin [a,b], J.-W. Choe [a], S.J. Lee [b], S.K. Noh [b,*], J.O. Kim [c], K.-S. Lee [d]

[a] Department of Applied Physics, Kyung Hee University, Yongin 449-701, Republic of Korea
[b] Nano Materials Evaluation Center, Korea Research Institute of Standards and Science, Daejeon 305-340, Republic of Korea
[c] Center for High Technology Materials, University of New Mexico, Albuquerque, NM 87106, United States
[d] Convergence Components & Materials Research Laboratory, Electronics and Telecommunications Research Institute, Daejeon 305-700, Republic of Korea

ARTICLE INFO

Article history:
Received 14 November 2013
Received in revised form
14 February 2014
Accepted 21 February 2014
Available online 12 March 2014

Keywords:
Quantum dot in double well
Asymmetric quantum well
Photoresponse spectra
Infrared photodetector

ABSTRACT

A triple-band mid-/far-infrared (MIR/FIR) photodetector tunable by polarity is demonstrated by asymmetric quantum dot-in-double-well (DdWELL) structure that exhibits unique photoresponse (PR) transitions. In contrast to the MIR2 band with no dependence, the two MIR1/FIR PR bands are blue/red-shifted by the bias voltage, and the MIR2-FIR dual-band spectrum changes to a single-band feature due to the polarity. A four-level energy band model is proposed for the transition scheme, and the electric field dependence of the FIR band numerically calculated by a simplified DdWELL structure is in good agreement with the experimental PR spectra.

1. Introduction

Unique features of quantum dots (QDs) make it possible to apply them to exotic electro-optic devices, such as single photon emitters [1], single electron transistors [2], terahertz (THz) devices [3], and various quantum detectors [4–7]. In these, the most successful device may be quantum-dot infrared photodetector (QDIP) whose imaging camera is presently near at hand [7–14]. In succession to realization of focal-plane array (FPA) detectors based on InAs/GaAs QDs, dual- and multi-band mid-/far-infrared (MIR/FIR) detectors using InAs/InGaAs quantum dot-in-a-well (DWELL) structures were reported [11–13]. Recently, we demonstrated a monolithically integrated plasmonic [320 × 256]-FPA QDIP camera, which showed wavelength selectivity and device performance enhanced by the surface plasmon that was generated at the interface between a metal with two-dimensional hole array and the FPA-QDIP [14]. It showed spectral-resonant coupling of the surface plasmon with infrared absorption in the QDs as an important step towards biomimetic vision of multi-color infrared imaging, the so called *infrared retina* [7].

It has been experimentally proven that QDIPs possess the fundamental ability to achieve the highest infrared detector performance if the QD array has optimal band structure and size uniformity [15]. However, there remains a strain problem arising from the inherent lattice mismatch between the InAs QDs and InGaAs cap layers, which induces a minor loss of quantum efficiency. As a modified approach to minimize strain accumulation during QD stacking, a quantum dot-in-double-well (DdWELL) structure [7] was proposed, in which InAs QD *ensembles* were positioned in a combined quantum well composed with two kinds of cap layers of InGaAs and GaAs in order to lower the overall indium composition of the well. This double well structure may be the best compromise to maximize the quantum confinement, keeping QD shape and reducing intermixing of species. The basic properties of the DdWELL structure stacked up to 60 periods were lately confirmed [16], but clear understanding of the photoresponse (PR) transition scheme in the DdWELL QDIP is required for realization of emerging multi-color infrared imaging technology [14,17–19].

In this work, we report a tunable triple-band MIR/FIR QDIP embodied by an asymmetric DdWELL structure and the origin of PR transitions identified by bias-dependent spectral behaviors. A four-level energy band diagram was proposed for the transition scheme, and the electric field dependence was calculated via wavefunction simulation for a simplified DdWELL structure. The wavelength shift

---

* Corresponding author. Korea Research Institute of Standards and Science, 267 Gajeong-ro, Yuseong-gu, Daejeon 305-340, Republic of Korea. Tel.: +82 42 868 5125; fax: +82 42 868 5047.
E-mail address: sknoh@kriss.re.kr (S.K. Noh).

http://dx.doi.org/10.1016/j.cap.2014.02.019
1567-1739/

by the field strength and the spectra tuned by the polarity are discussed on the basis of four-level transition.

2. Experimental procedure

Fig. 1(a) presents device structure of a discrete n-i-n photodetector that is fabricated on a 30-period asymmetric InAs-QD/[InGaAs/GaAs]/AlGaAs DdWELL wafer grown by using molecular beam epitaxy (MBE). A 2.0-monolayer (ML) InAs QD *ensemble* was embedded in the upper combined well of $In_{0.15}Ga_{0.85}As$/GaAs, and each stack was separated by a 50-nm $Al_{0.1}Ga_{0.9}As$ barrier. Nominal thicknesses of InGaAs/GaAs layers were 1.0/4.0 nm and 1.0/6.85 nm for upper and lower wells, respectively, where the GaAs wells were asymmetrically designed. A pair of n^+-GaAs contact layers (1.25 μm) was prepared at the top and the bottom of the device for metallization, and a 50-nm AlAs layer for etch stop was deposited on GaAs buffer.

Each pixel had circular aperture of 300 μm in diameter, and the mesa cell ($410 \times 410\ \mu m^2$) was defined by shallow etching in order to minimize surface leakage. Well-defined QDs in DdWELL structure were demonstrated by the transmission electron microscope (TEM) image as shown in the inset of Fig. 1(b), and a strong emission of ~1.2 eV from the QD *ensemble* was confirmed by 300-K photoluminescence (PL) spectra as presented in Fig. 1(b). These indicate that the present device under study maintains excellent characteristics.

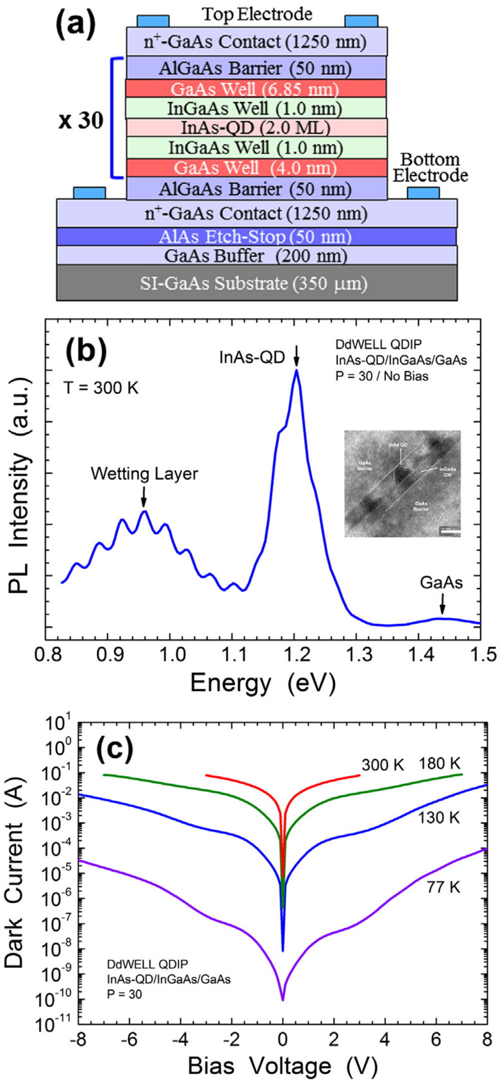

Fig. 1. (a) Device structure of DdWELL QDIP used in this study, and (b) room temperature PL spectrum taken under no bias with a TEM photograph showing well-defined QD image in the active layer. (c) Temperature dependence of the dark current–voltage characteristic curves.

PR measurements were performed in the spectral range of 3–13 μm (100–400 meV) by using a Fourier-transform infrared (FTIR) spectrometer (Nicholet 5700) and a low-noise preamplifier (Keithley 428). The signals were weighted by the response of the whole system including a source and a detector. The bias voltage was varied by a 0.2-V step in the range of ±12 V. Fig. 1(c) presents the temperature dependence of the dark current–voltage (I_D–V) characteristic curves tested in the measurable range of picoammeter used in this experiment, and no temperature dependence of PR spectra up to 100 K was confirmed. PR spectra discussed in this study were obtained at a temperature of 13 K.

3. Results and discussion

Representative PR spectra taken from the DdWELL QDIP under (a) forward and (b) reverse biases are displayed in Fig. 2. The forward spectra exhibit a minor peak around 5 μm and two distinctive peaks near 6.5 μm and 10 μm. Hereinafter, for convenience sake, we name the three peaks as mid-infrared 1 (MIR1), mid-infrared 2 (MIR2), far-infrared (FIR) in order, as denoted in the figures. (An additional faint peak around 4.2 μm will be mentioned later.) In the reverse spectra, two weak peaks appear around the positions equivalent to those of the forward MIR1 and MIR2, and a strong peak corresponding to FIR is found near 9 μm that is blue-shifted by 1–2 μm from the forward FIR position. It is very interesting that MIR2 band shows no wavelength shift in the full bias range, which is opposed to MIR1 and FIR bands with individual dependences at both bias polarities, as plotted in Fig. 3. In addition, the forward PR spectra having two dominant peaks are changed to a single-band profile with a major FIR peak at reverse bias, which may be closely correlated with asymmetric band [20,21].

Fig. 3 presents the transition energies of MIR1, MIR2, and FIR plotted as a function of the electric field. (Bold and normal symbols denote major and minor peaks, respectively.) The electric field strength was estimated by applied bias voltage and total thickness of the active layer of the device. Here, we assume that the electric field is uniform on average in the device. As the strength increases at each polarity, MIR1/FIR peaks are almost linearly blue-/red-shifted with individual rates, in striking contrast to MIR2 that shows no dependence. The blue-shift rate of MIR1 is almost the same as 1.0–1.1 meV/(kV/cm) at either polarity. On the other hand, the red-shift rate of forward FIR (~0.3 meV/(kV/cm)) is approximately three times higher than that of the reverse FIR (~0.1 meV/(kV/cm)), which is a result of the abrupt spectral change by biasing. The single-band feature at reverse bias is supposed to arise from involvement of quasi-bound states related to the asymmetric GaAs wells [20,21]. Based on these transition behaviors, a four-level system is proposed for the energy band model to suggest the origin of PR bands in DdWELL QDIPs.

Schematic energy-band diagrams under forward (left) and reverse (right) biases are depicted in Fig. 4. (Solid lines denote major transitions showing strong PR signals, and dashed/dotted lines are for minor ones with weak/negligible intensity.) We introduce three sublevels, a ground state in QD (E_{D0}) and two excited states in QW (E_{W1}, E_{W2}). The three PR peaks (MIR1, MIR2, FIR) designated in Fig. 2 correspond to transitions of [$E_{W1} \rightarrow E_C$], [$E_{D0} \rightarrow E_{W1}$], and [$E_{W1} \rightarrow E_{W2}$], respectively. Here, E_C denotes the continuum state lying just above the conduction band edge of the AlGaAs barrier. An additional faint peak around 4.2 μm shown in